CHEMBIOCHEM

DOI: 10.1002/cbic.200900331

Passage of Trojan Peptoids into Plant Cells

Kai Eggenberger,[a] Esther Birtalan,[b] Tina Schröder,[b] Stefan Bräse,[b] and Peter Nick*[a]

Efficient drug delivery is essential for many therapeutic applications. In this context, Trojan peptoids have attracted attention as powerful tools to deliver bioactive molecules into living cells. Certain cell-penetrating peptides, peptide mimetics, and peptoids have been shown to be endowed with a transport function and the structural features of this function have been characterized. However, most of the research has been done by using mammalian cell cultures as model organisms and the actual cellular mechanism of membrane passage has not been elucidated. Plant cells, which are encased in a cellulosic cell wall and differ in membrane composition, represent an alternative experimental system to address this issue, but so far, have attracted only little attention for both peptide- and peptoid-based carrier systems. Moreover, efficient delivery of nonproteinaceous bioactive macromolecules into living plant cells could complement genetic engineering in biotechnological applications, such as metabolic engineering and molecular farming. In the present study, we investigated carrier peptoids with or without guanidinium side chains with regard to their uptake into plant cells, the cellular mechanism of uptake, and intracellular localization. We can show that in contrast to polyamine peptoids (polylysine-like) fluorescently labeled polyguanidine peptoids (polyarginine-like) enter rapidly into tobacco BY-2 cells without affecting the viability of these cells. A quantitative comparison of this uptake with endocytosis of fluorescently labeled dextranes indicates that the main uptake of the guanidinium peptoids occurs between 30–60 min after the start of incubation and clearly precedes endocytosis. Dual visualization with the endosomal marker FM4-64 shows that the intracellular guanidinium peptoid is distinct from endocytotic vesicles. Once the polyguanidine peptoids have entered the cell, they associate with actin filaments and microtubules. By pharmacological manipulation of the cytoskeleton we tested whether the association with the cytoskeleton is necessary for uptake, and observed that the actin inhibitor latrunculin B as well as the microtubule inhibitor oryzalin impaired uptake and intracellular spread of the guanidinium carrier to a certain extent. These findings are discussed with respect to the potential mechanisms of uptake and with respect to the potential of Trojan peptoids as tools for metabolic engineering in plant biotechnology.

Introduction

It has been well known for several decades, that some peptides with basic amino acid residues are taken up rapidly by mammalian cells in culture.[1–9] Initial assays suggested that these peptides could directly traverse the plasma membrane by an unknown mechanism, independently of classical receptor-mediated pathways. Some of these peptides were discovered as basic domains responsible for the translocation of naturally transduced proteins and were therefore referred to as protein transduction domains (PTDs).[10–12] They can transport covalently attached cargo molecules of diverse chemical nature (oligonucleotides, proteins, fluorophores, and even liposomes or nanoparticles) into target cells. In parallel, many synthetic peptides composed of α-amino acids have been discovered or designed that mediate membrane passage. Peptides sharing the ability to cross the membrane barrier of living cells independently of receptor-mediated endocytosis are now conventionally designated as cell-penetrating peptides.[10–12] The most important structural features for the efficiency of CPP uptake appear to be: 1) the short size, 2) high content of cationic residues, and 3) variable spacing between the charges. In contrast, the backbone conformation does not seem to play a critical role.[10–12] However, the bioavailability of CPPs is limited by proteolysis in vivo. Therefore, short peptide mimetics with modified backbones, carrying basic functionalities, such as amino or guanidinium groups, might serve as a valuable alternative to CPPs because of their enhanced stability in vivo. Proteolytically stable β peptides, for instance, have been under intensive investigation during recent years,[13] and were shown to be efficiently internalized by cultured mammalian cells.[3]

Peptoids (oligo-*N*-alkylglycines) are stable against proteases, similar to β peptides, but usually are less prone to aggregation.[3,14,15] In contrast to both α and β peptides, the side chains of peptoids are attached to the nitrogen atom instead of the carbon, therefore, they lack hydrogen-bonding potential, which prevents backbone-driven aggregation and thus increases bioavailability. These peptide mimetics have been successfully synthesized and used as effective, water soluble, nontoxic molecular transporters for intracellular drug delivery or as molecular probes for bioconjugation.[16–21] Peptoids with guanidinium head groups attached to alkyl chains have also been

[a] *K. Eggenberger, Prof. Dr. P. Nick*
Institute of Botany 1, University of Karlsruhe
Kaiserstrasse 2, 76128 Karlsruhe (Germany)
Fax: (+49) 721-608-4193
E-mail: peter.nick@bio.uni-karlsruhe.de

[b] *E. Birtalan, Dr. T. Schröder, Prof. Dr. S. Bräse*
Institute of Organic Chemistry, University of Karlsruhe
Fritz-Haber-Weg 6, 76131 Karlsruhe (Germany)

used to mimic peptide hormones, antibiotics, and receptor ligands.[16–20]

Although the general setup of the plasma membrane is similar over the different kingdoms, differences in the composition of both proteins and lipids do exist. For instance, lipid rafts, specific domains of the plasma membrane where signaling proteins are concentrated in a lipid environment that is enriched in saturated fatty acids, are characteristic for animal cells, but are still a matter of debate in plant cells.[22–24] On the other hand, the content of unsaturated fatty acids can be strongly up-regulated in an adaptive manner in response to environmental triggers, such as cold stress.[24] Since these changes concern the fluidity of the plasma membrane, it is expected that they influence the uptake of Trojan peptoids.

Results and Discussion

So far, only peptide based carrier systems have been successfully employed in plant cells,[25] but at least to our knowledge, the introduction of peptoid based carrier systems into plant cells has not been attempted. This is not a matter of mere academic interest; if Trojan peptoids can be used as tools to introduce large cargoes into living plant cells, this would be of great use for plant metabolic engineering and molecular farming applications, especially for organic precursor molecules that are difficult to generate by means of genetic engineering. We, therefore, ventured to study whether Trojan peptoids can enter plant cells and, if so, by what cellular mechanism. To address these questions we had to combine chemical approaches (design and synthesis of fluorescently-labeled Trojan peptoids) with molecular plant cell biology (tissue culture, fluorescently tagged cell lines).

The peptoids were synthesized on solid phase by using a Rink amide resin by cycles of monomer addition and washing of unbound substrate. Peptoid TS-063 (Scheme 1 A), as a representative of the polyamine (polylysine-like) peptoids, was obtained as a red–brown solid and labeled with rhodamine with absorption maxima at 200, 257, 354, and 547 nm. Peptoids TS-165 (Scheme 1 B) and EB-220 (Scheme 1 C) were selected as representatives of the polyguanidine (polyarginine-like) peptoids and were coupled to carboxyfluorescein and rhodamine B, respectively.

The behavior of the three peptoids was followed over the first 20 h after addition to tobacco BY-2 cells by epifluorescence microscopy in combination with optical sectioning by using the apotome technology. This approach excludes any fluorescent signal that does not originate from the focal plane. By shifting the focus in the *z* axis through the cell it is thus possible to record *z* stacks of images that are void of any nonfocal signal. This approach ensures that a fluorescent signal collected from the interior of the cell indeed originates from the cytoplasm and is not contaminated by nonfocal signals from the surface of the cell. All peptoids first attached to the apoplast before they entered the target cells (TS-165, Figure 1 A; TS-063, Figure 1 C). While this attachment was observed at the same time for all three peptides, the time span after which the first intracellular signal became detectable differed greatly. The TS-165 signal was observed to become progressively intracellular already 45 min after the first contact, and had accumulated in almost all cells within the first 2 h (Figure 1 A). The uptake of EB-220 was even faster and led to a redistribution of the signal in a filamentous pattern extending through the entire cytoplasm already within the first 20 min of incubation (Figure 1 D). In contrast, at least 6 h incubation was required for TS-063 before the first intracellular signal became manifest. After 20 h incubation the TS-165 peptoid was released into the vacuole in the majority of cells (Figure 1 A). However, at this time point only very few vesicular structures could be detected with the TS-063 peptoid (Figure 1 C). Thus, the two polyguanidine peptoids, TS-165 and EB-220, showed rapid translocation into plant cells as opposed to the polyamine peptoid, TS-063.

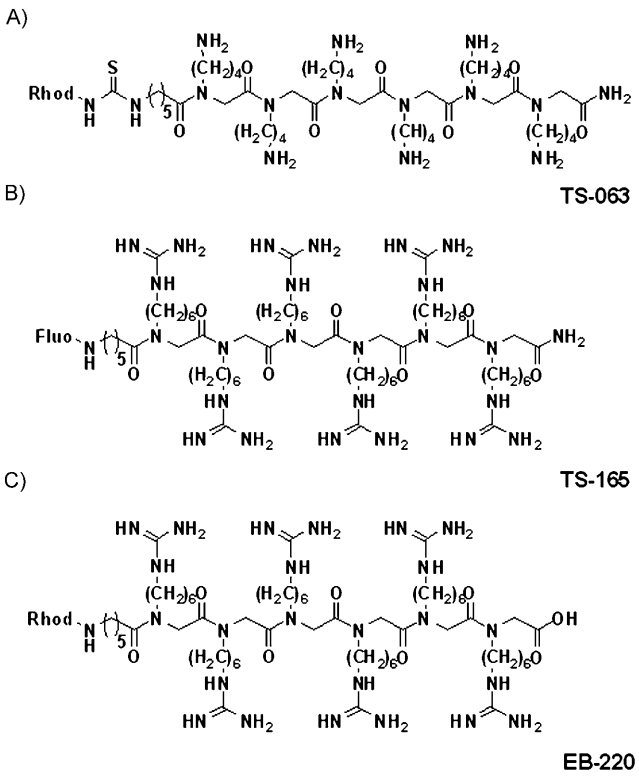

Scheme 1. Structure of the Trojan peptoids used in this study. A) The polylysine-like Trojan peptoid TS-063 was tagged with rhodamine (Rhod) as fluorescent marker, B) the polyarginine-like Trojan peptoid TS-165 was tagged with carboxyfluorescein (Fluo) as marker, and C) EB-220 was tagged with rhodamine.

To characterize the rapid uptake of polyguanidine peptoids and its underlying mechanisms in more detail we developed a microscopic assay to quantify the passage of the Trojan peptoid TS-165 in relation to the fluorescently labeled dextrane FD-4, as inert reference cargo. TS-165 first attached to the cell before it progressively and rapidly redistributed to the cytoplasm (Figure 1 A). In contrast, FD-4 was endocytotically transported into the cell from the start of incubation, however, at a much slower pace and without the apoplastic accumulation that was characteristic for the uptake of the Trojan peptoids (compare Figure 1 B and 1 A). To follow the uptake of both TS-

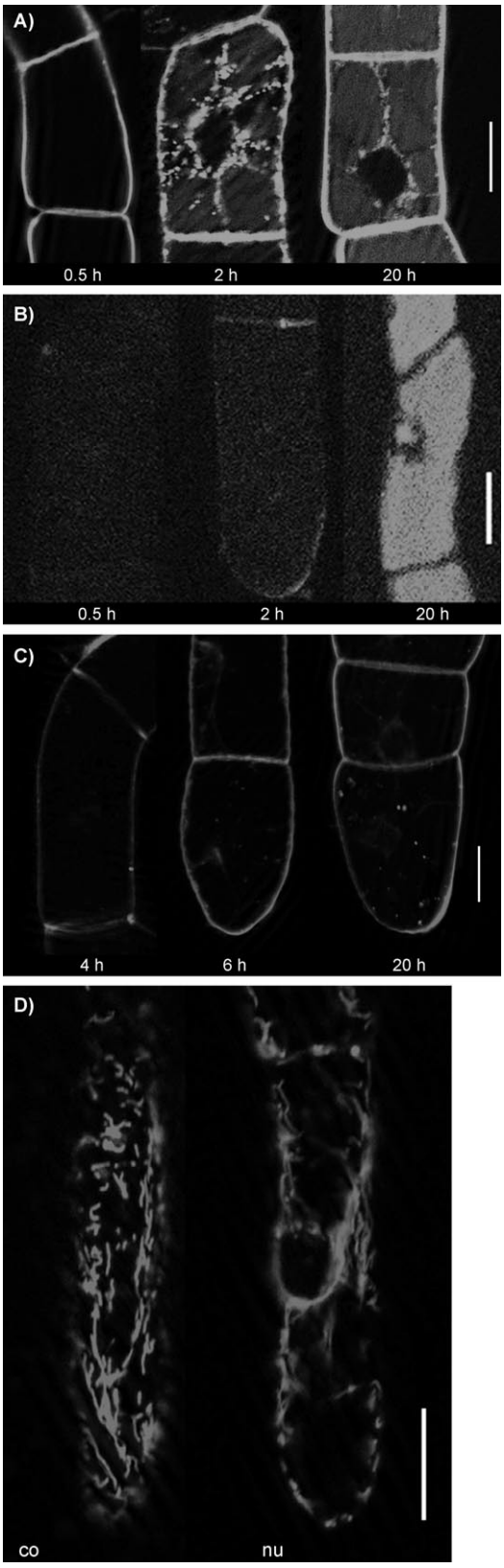

Figure 1. Individual tobacco BY-2 cells at different times after incubation with: A) the Trojan peptoid TS-165, B) fluorescently labeled dextrane FD-4, C) TS-063, or D) EB-220, in the cortical (co) plane and in the nuclear (nu) plane of the cell. The incubation time for EB-220 was 20 min; scale bar: 20 μm.

165 and FD-4 over time we quantified the intracellular fluorescence intensity relative to the signal in the medium. This time course confirmed the qualitative impression that TS-165 enters extremely rapidly to establish a high plateau within the first hour of incubation (Figure 2). Already after 30 min, the uptake

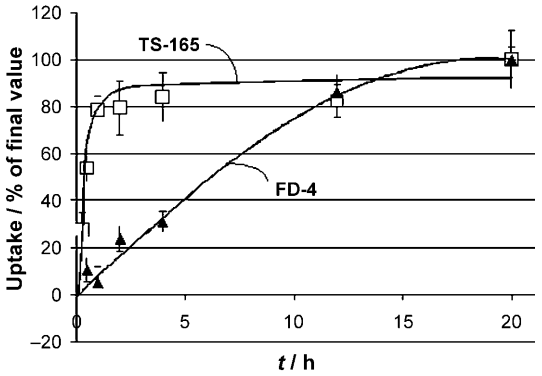

Figure 2. Time course of uptake for the Trojan peptoid TS-165 as compared to the fluorescently labeled dextrane FD-4 into tobacco BY-2 cells. Each data point represents the mean of 167 to 245 individual cells from two independent experimental series.

had reached 50% of this plateau. In contrast, 5–10 h elapsed before FD-4 accumulated to around 50% of its final level. Furthermore, the total amount of TS-165 fluorescence after 20 h incubation had more than threefold increased in comparison to the reference substance FD-4 (Figure 3).

FD-4 as hydrophilic cargo can neither pass the membrane by diffusion nor are any carriers known that allow membrane passage of this cargo. The uptake of FD-4, therefore, mirrors the activity of the endocytotic machinery. Thus, the observed time courses demonstrate very clearly that endocytosis cannot account for the extremely rapid uptake of the polyguanidine peptoid TS-165 into plant cells.

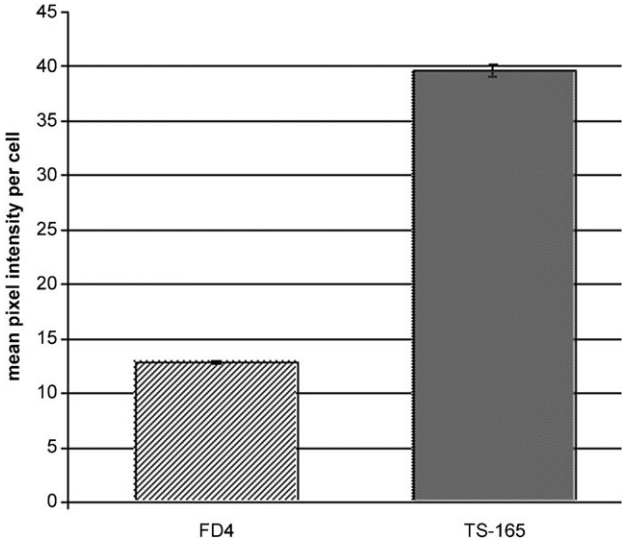

Figure 3. Amount of FD4 and TS-165 taken up by the cells during an incubation period of 20 h. The data points represent the mean of 227 individual cells for FD4 and 188 individual cells for TS-165.

Once TS-165 had entered the target cell it became manifest in form of small vesicles. To test whether these vesicles represent so-called endosomes, we counterstained the vesicles with the fluorescent endosomal marker FM4-64[26] (Figure 4), but observed that the majority of the vesicular structures labeled by TS-165 differed from those visualized with FM4-64. Thus, only a small fraction of TS-165 seems to be associated with classical endosomes. To test this on the functional level, we incubated the cells with either TS-165 or the endocytotic test cargo FD-4 in the presence of 33 μM of the endocytosis inhibitor Wortmannin[27] for 2 h and quantified the uptake as described above. The uptake of TS-165 was only marginally reduced (from a relative value of 16.3 ± 1.9 to 14.4 ± 0.5, i.e., by 13%) whereas the uptake of FD-4 was strongly reduced (from a relative value of 11.1 ± 0.6 to 6.8 ± 0.6, i.e., by 40%); this is consistent with the published values for the inhibition of endocytosis in BY-2 cells by Wortmannin.[27]

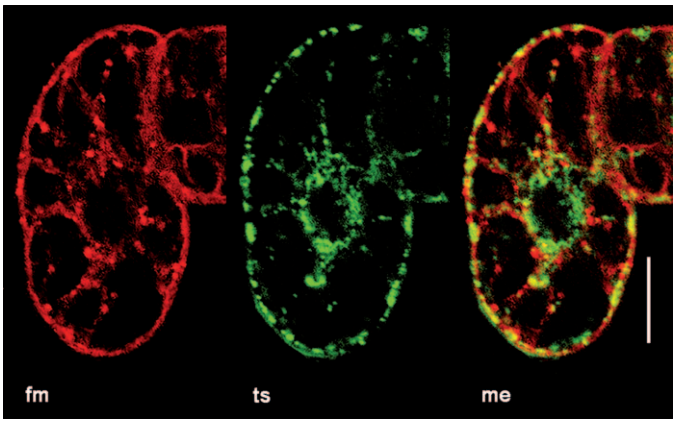

Figure 4. Simultaneous visualization of the endosomal marker FM4-64 (fm) and TS-165 (ts) and merge (me) of the two signals in the central nuclear plane of individual tobacco BY-2 cells; scale bar: 20 μm.

To assess whether the vesicles labeled by TS-165 are tethered to the cytoskeleton, we visualized actin filaments and microtubules in tobacco cells that had been incubated with TS-165 (Figure 5). Optical sections through the cortical region of tobacco BY-2 cells showed that the vesicular structures labeled by TS-165 decorated actin filaments comparable to beads on a string (Figure 5A), although a part of these vesicles could not be assigned to individual microfilaments. Similarly, cortical microtubules were decorated by TS-165 vesicles (Figure 5B), but again some vesicles were found without an obvious association with microtubules. Thus, the vast majority of vesicles were observed to be tethered to either microtubules or actin filaments.

This association with the cytoskeleton might be a downstream event related to the storage or anchoring of Trojan peptoids after uptake has taken place. On the other hand, it might be relevant for the uptake process per se. We, therefore, treated the cells with either latrunculin B, which is an inhibitor of actin, or with oryzalin, which is a specific inhibitor of plant microtubules. Both compounds act by sequestering either monomers or dimers, respectively, such that the polymers are eliminated due to their innate turnover.[28,29] After pretreatment of the target cells with the anticytoskeletal drugs, overnight, we tested whether the cells were able to take up the polyguanidine peptoid TS-165. While both latrunculin B and oryzalin caused a degradation of the actin filaments or microtubules in a similar fashion, they differed in their ability to impair the passage of TS-165 into the target cells. When the inhibition of uptake was quantified, latrunculin B was found to decrease the uptake of TS-165 into cells by 13.6% (from a relative value of 41.0 ± 0.6 to 35.4 ± 0.7), whereas oryzalin inhibited by 22.2% (from a relative value of 41.0 ± 0.6 to 32.3 ± 1.1). Thus, although both actin filaments and microtubules appear to influence the uptake of Trojan peptoids, microtubules have a slightly stronger involvement as compared to actin filaments. These findings concur with the visual evaluation of the colocalization experiments that already suggested a slightly higher preference of the TS-165 vesicles for microtubules (Figure 5).

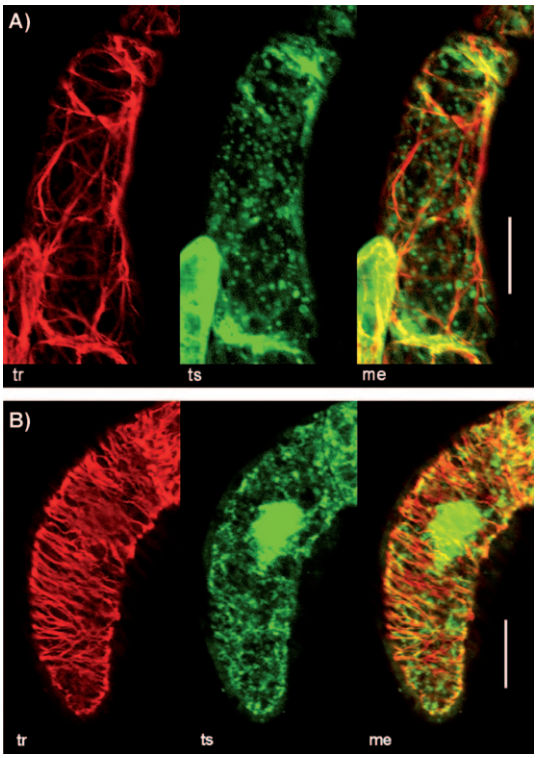

Figure 5. Dual visualization of the Trojan peptoid TS-165 with: A) actin filaments, and B) microtubules; tr: signal for actin filaments (in A) and microtubules (in B); ts: signal for TS-165; me: merge of both signals; scale bar: 20 μm.

Our results demonstrate that Trojan peptoids are suitable carrier systems to deliver cargoes of interest into plant cells. While both polyamine and polyguanidine peptoids were able to enter the cells, they differ strongly with respect to their kinetic properties. The size of the peptoids seems to be irrelevant with regard to the uptake kinetics since the slower polyamine peptoid TS-063 is considerably smaller than the fast polyguanidine peptoids TS-165 and EB-220. The uptake of the polyguanidyl peptoid TS-165 could be clearly delineated from receptor-mediated endocytosis, because it proceeds at a much faster rate as compared to fluorescently labeled dextrane FD-4

(Figure 2), because most of the intracellular TS-165 is localized outside canonical endosomes (Figure 4). In addition, the uptake of TS-165 is only marginally inhibited by the endocytosis inhibitor Wortmannin, in contrast to the endocytotic test cargo FD-4. Furthermore, the total amount of fluorescent test cargo delivered into the cell by TS-165 over a span of 20 h is more than three times the amount of endocytotically acquired FD-4 (Figure 3).

The polyguanidyl peptoid TS-165 associates with both actin filaments and microtubules (Figure 5), and this association with the cytoskeleton is relevant for either the uptake itself or for the recycling of the uptake machinery, since passage of TS-165 can be impaired but not disabled by inhibitors of actin and microtubule assembly. We show for the first time that, despite the structural differences between plant and animal membranes, Trojan peptoids can be used as efficient tools to permeate the plasma membrane of plant cells independently of endocytosis. This indicates that the membrane passage of these peptoids is based upon mechanisms that have been conserved throughout evolution and that seem to be dependent on the chemical nature of the peptoids rather than on their size. To our knowledge, this is the first report for a role of the cytoskeleton in the uptake of Trojan peptoids, and it remains to be elucidated whether this represents a plant-specific feature or whether the cytoskeleton is involved in membrane passage in other systems as well. Future research will be dedicated to the use of functionalized derivatives of Trojan peptoids to tailor specific metabolic reactions within tobacco cells as a step towards metabolic engineering of pathways that are difficult to design by means of gene technology.

Experimental Section

Synthesis and characterization of the Trojan peptoids

Synthesis of the monomeric units: For the synthesis of the monomeric units see refs. [17, 30, 31].

Solid-phase synthesis: Solid-phase reactions greatly facilitated the synthesis as the growing oligomer attached to a solid support can easily be purified from excess reactants by washing the resin with the appropriate solvents and subsequent filtration. The protection of free amino groups with Fmoc has been well established as this protecting group can be quantitatively removed under mild conditions in a short reaction time. Rink amide resin was chosen as a solid support due to its stability at ambient conditions, the ease of the first coupling step, and good cleavage conditions. Furthermore, the reaction conditions are the same for attaching the first building block to the resin and the following coupling cycles. After removal of the Fmoc group that protects the amino-functionalized resin (with 20% piperidine in DMF), an activated Fmoc-protected monomer was coupled to the solid phase via a peptide bond. In this reaction, bromo-tris(pyrrolidino)phosphonium-hexafluoro-phosphate (PyBrOP) was used to generate an activated ester and *N*,*N*-diisopropylethylamine (DIPEA) was added to enhance the rate of ester formation. For the microwave-assisted reactions HOBt and DIC were used as coupling reagents. The Fmoc group was removed with piperidine solution to yield the coupled monomer for the attachment of the next building block. Coupling of the monomers to the growing peptoid chain proceeded under the same conditions as the attachment of the first building block to the solid support. All reaction procedures were succeeded by repetitive washing that ended with a solvent, in which the resin was swelled to expose its reactive sites to the next reagents. The cycles of coupling and deprotection were repeated until a peptoid of the desired length was obtained. Furthermore, microwave-assisted synthesis[18] was performed to shorten coupling time. For milder cleavage conditions PL Cl-Trt-Cl resin was used. The activation and deprotection steps were carried out as described above.

Synthesis of peptoids (general procedure A1): The amino-functionalized Rink amide resin (0.51 mmol, 1 equiv) was covered with five times its volume of dichloromethane and swelled for 30 min. After removal of the solvent, the Fmoc protection group of the linker amine was removed by incubation with piperidine solution (20% in DMF, 6 mL) for 2 min. This procedure was repeated twice. For the coupling step, the crystalline building block (1.53 mmol, 3 equiv) was added to the resin, followed by PyBrOP (1.02 mmol, 2 equiv) and DIPEA (2.04 mmol, 4 equiv). The solid was suspended in dichloromethane (6 mL) and shaken for 24 h. Then, the solution was removed and the resin was washed according to a standard procedure by using a sequence of MeOH/DMF/MeOH (2×), THF/MeOH/THF/MeOH/THF/pentane, dichloromethane/*n*-pentane (3×) and pentane. Finally, the resin was dried in vacuo (2 Pa) for 48 h. Coupling of the respective monomers to the peptoid chain proceeded under identical conditions as the attachment of the first building block to the solid support. All reaction procedures were carried out by repetitive cycles of coupling and deprotection until a peptoid of the desired length was obtained.

Microwave-assisted synthesis (general procedure A2): The resin (0.264 mmol, 1 equiv) was covered with five times its volume of dried DMF and swelled for 30 min. Meanwhile the building block (0.422 mmol, 1.6 equiv) and DIPEA (1.69 mmol, 6.4 equiv) were mixed in dried DMF (4 mL). After removal of the solvent the reaction solution was added to the resin and shaken for 20 h. Then, the solution was removed, and the resin was washed according to a standard procedure by using a mixture of dichloromethane/MeOH/DIPEA (17:2:1; 2) and by using a sequence of dichloromethane/DMF/dichloromethane (5×). Finally, a small amount of the resin was dried in vacuo (2 Pa) for 24 h to determine the loading after standard protocols (loading of resin: 0.35 mmol g^{-1}). For further coupling steps the Fmoc protection group was removed by incubation with piperidine solution (20% in DMF, 3 mL) for 5 min. This procedure was repeated twice. Then the building block (0.21 mmol, 3 equiv), HOBt (0.21 mmol, 3 equiv), and DIC (0.21 mmol, 3 equiv) were dissolved in DMF (2.1 mL, 0.1 M) and added to the resin (0.07 mmol, 1 equiv). The resin was not dried after the reactions. The reaction was performed in a CEM microwave (20 min reaction time, 50 °C). All reaction procedures were carried out by repetitive cycles of coupling and deprotection until a peptoid of the desired length was obtained.

Attachment to the solid phase and construction of the peptoids

Hexamer at Rink amide linker:[30] As described in general procedure A1, the Rink amide resin was treated with *N*-(4-*tert*-butoxycarbonylaminobutyl)-*N*-(9*H*-fluorene-9-ylmethoxycarbonyl)amino acetic acid. This reaction was repeated five times to obtain the resin-bound hexamer as a beige resin in a yield of 0.19 g; loading of the hexamer: 0.33 mmol g^{-1}.

Nosyl-protected hexamer at Rink amide linker: As described in general procedure A1 the Rink amide resin was treated with *N*-(9*H*-fluorene-9-ylmethoxy-carbonyl)-*N*-{6-(2′-nitrobenzenesulfonyl-amino)-hexyl}amino acetic acid. This reaction was repeated five times to

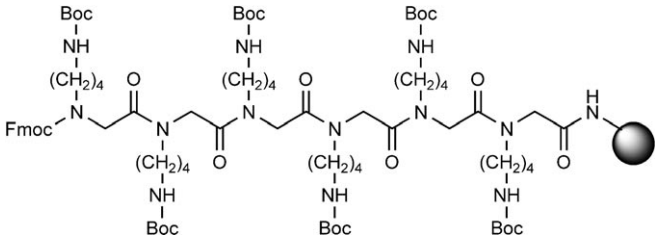

obtain the resin-bound hexamer as a yellow resin in a yield of 0.17 g; loading of the hexamer: 0.28 mmol g^{-1}.

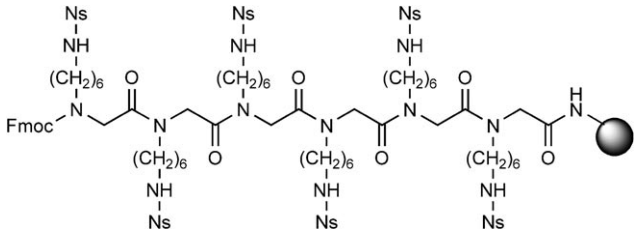

Nosyl-protected hexamer at Cl-Trt-Cl linker: As described in general procedure A2 the Cl-Trt-Cl resin was treated with *N*-(9*H*-fluorene-9-ylmethoxy-carbonyl)-*N*-{6-(2′-nitrobenzene-sulfonyl-amino)hexyl}-amino acetic acid. This reaction was repeated five times to obtain the resin-bound hexamer as a yellow resin.

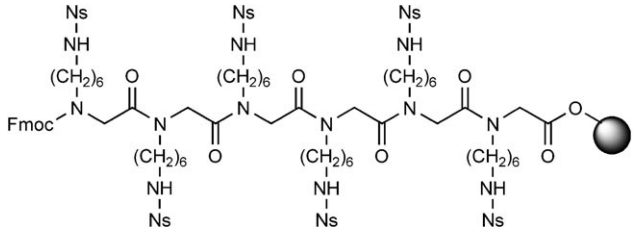

Labeling (general procedure B1): Prior to attaching the fluorophore to peptoids, *N*-Fmoc-aminohexanoic acid was coupled as a spacer to limit steric hindrance between marker and transporter. The immobilized peptoid was first deprotected as described in general procedure A1. This step was repeated twice. For the coupling step of the spacer, *N*-Fmoc-aminohexanoic acid (0.25 mmol, 3 equiv) was added to the resin. PyBrOP (0.16 mmol, 2 equiv) and DIPEA (0.33 mmol, 4 equiv) were added as activating reagents and the suspension was gently agitated for 24 h in dichloromethane (6 mL). Then the solvents were removed and the resin was washed according to the standard procedure (see general procedure A1). Finally, the resin was dried in vacuo for 48 h. After the resin was re-swelled and deprotected with piperidine solution (as described in general procedure A1) the fluorophores 5(6)-carboxyfluoresceine and rhodamine B isothiocyanate (0.25 mmol, 3 equiv) were attached. To activate 5(6)-carboxyfluoresceine and rhodamine B isothiocyanate the fluorophores (0.25 mmol, 3 equiv) were mixed with HOBt (0.25 mmol, 3 equiv) in a 50 mL flask, followed by addition of dichloromethane/DMF (1:1, *v/v*; 2 mL). Then DIC (0.25 mmol, 3 equiv) was added and the mixture was shaken for 20 min at room temperature, and was then added to the prepared resin derived from general procedure B. The suspension was agitated for 5 h.

Microwave-assisted synthesis (general procedure B2): The immobilized peptoid was first deprotected as described in general procedure A2. For the coupling step of the spacer *N*-Fmoc-aminohexanoic acid (0.21 mmol, 3 equiv), HOBt (0.21 mmol, 3 equiv), and DIC (0.21 mmol, 3 equiv) were dissolved in DMF (2.1 mL, 0.1 M) and added to the resin (0.07 mmol, 1 equiv). The reaction was performed in a CEM microwave (20 min reaction time, 50 °C). After the resin was washed and Fmoc deprotected, as described in general procedure A2, rhodamine B (0.21 mmol, 3 equiv), HOBt (0.21 mmol, 3 equiv), and DIC (0.21 mmol, 3 equiv) were dissolved in DMF (2.1 mL, 0.1 M) and added to the resin. The reaction was performed in a CEM microwave (20 min reaction time, 50 °C).

Labeling of the immobilized peptoids with fluorophores: Prior to attaching the label to peptoids, *N*-Fmoc-aminohexanoic acid was coupled as a spacer to inhibit steric hindrance between label and transporter.

Fluorophore-labeled hexamer:[30] As in general procedure B1 the hexapeptoid was treated with rhodamine B isothiocyanate for 5 h, and afterwards washed and dried as described in general procedure B1; loading: 0.29 mmol g^{-1}.

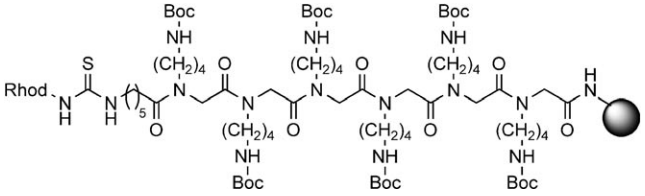

As in general procedure B1 the nosyl-protected hexapeptoid was treated with 5(6)-carboxyfluoresceine for 5 h and afterwards washed and dried as described in general procedure B1. The labeled peptoid was obtained in a yield of 0.09 g; loading: 0.27 mmol g^{-1}.

As in general procedure B2 the nosyl-protected hexapeptoid was treated with rhodamine B for 30 min and afterwards washed.

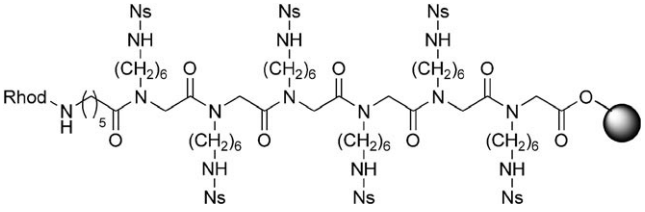

Nosyl deprotection (general procedure C1): For the deprotection of the nosyl-functionalized amino groups, the resin (0.09 mmol, 1 equiv) was covered with dichloromethane (3 vol. according to the initial resin volume) and swelled for 30 min. After the solvent was removed by filtration, the resin was deprotected by treatment with a solution of 2-mercaptoethanol/DBU (0.3 M diaza-[5.4.0]-bicycloundecene in 2 mL DMF). The suspension was shaken for 45 min, the solvents were removed and the deprotection step was repeated twice. The resin was washed and dried, as outlined in general procedure A1.

Microwave-assisted synthesis (general procedure C2): For the deprotection of the nosyl-functionalized amino groups, the resin

(0.07 mmol, 1 equiv) was covered with a solution of 2-mercaptoethanol/DBU (0.3 M diaza-[5.4.0]-bicycloundecene in 3 mL DMF). The reaction was performed in a CEM microwave (20 min reaction time, 50 °C). The resin was washed as outlined in general procedure A2.

Guanidinylation of side-chain amines (general procedure D1): After the nosyl deprotection of the side chain amines, as outlined in general procedure C1, the resin was covered with five times its volume of dichloromethane and swelled for 30 min. After removal of the solvent, 1*H*-pyrazol-1-carboxamidine (1.60 mmol, 10 equiv) was added to the resin, followed by DIPEA (1.60 mmol, 10 equiv) and DMF (5 mL). The suspension was shaken for 24 h. The solvents were removed and the resin was washed and dried, as outlined in general procedure A1.

Microwave-assisted synthesis (general procedure D2): After the nosyl deprotection of the side chain amines as outlined in general procedure C2, the resin was covered with a solution of 1*H*-pyrazol-1-carboxamidine (0.70 mmol, 10 equiv), DIPEA (0.70 mmol, 10 equiv) and DMF (2.00 mL). The reaction was performed in a CEM microwave (20 min reaction time, 50 °C). The resin was washed as outlined in general procedure A2.

Deprotection of the nosyl-protected side chains and treatment with guanidine groups

Fluorophore-labeled hexamer: The nosyl-protected hexapeptoid was deprotected as described in general procedure C1, followed by treatment of the free amines to give the resin bound guanidine peptoid in a yield of 0.07 g; loading: 0.32 mmol g^{-1}.

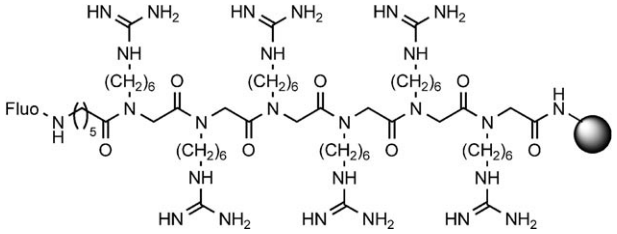

Deprotection of the nosyl-protected side chains and treatment with guanidine groups

Fluorophore-labeled hexamer: The nosyl-protected hexapeptoid was deprotected as in general procedure C2, followed by treatment of the free amines to give the resin bound guanidine peptoid.

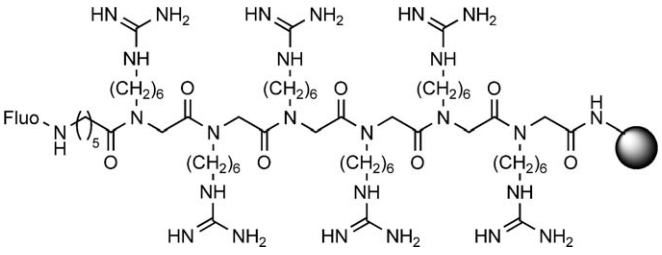

Cleavage and isolation (general procedure E1): To cleave the peptoid from solid support, the resin was transferred into a flask (25 mL) and covered with a solution of TFA/TIS (95:5, *v/v*; 1 mL). The suspension was gently agitated at room temperature for 3 h under argon atmosphere. Then, the solution was filtered, and the resin was rinsed with TFA (2×3 mL). In order to isolate the product, cold diethyl ether (50 mL, −78 °C) was added to the solution. After gentle agitation the peptoid precipitated. It was filtered off and dried in vacuo.

Microwave-assisted synthesis (general procedure E2): To cleave the peptoid from solid support, the resin was covered with a solution of TFA/dichloromethane (1:99, *v/v*; 2 mL). The suspension was gently agitated at room temperature for 2 h. Then, the solution was filtered and the resin was rinsed with cleavage solution (2× 3 mL). In order to isolate the product, cold diethyl ether (20 mL, −78 °C) was added to the solution; no precipitation occurred. The solvent was evaporated and the substance was lyophilized.

Cleavage and isolation of the carriers

Rhod-{4,4,4,4,4,4}-NH_2 (TS-063): As described in general procedures A1, B1, and E1, the product was obtained as a red–brown solid; yield: 88 mg (39% over 9 steps). TLC: CH_3CN:H_2O (1:1) + TFA (1 drop), RP-18 F_{254} TLC-plate; $R_f = 0.42$; UV/Vis (CH_3OH): λ_{max} ($\log\varepsilon$) = 200 (4.7), 257 (3.8), 354 (3.0), 547 (4.0); MS (FAB (LR), matrix: glycerine), *m/z* (%) [Norm: 899]: 1399 (76) $[M-Cl]^+$, 1271 (22) $[M-\text{monomer}]^+$, 1144 (18) $[M-2\ \text{monomers}+H]^+$, 1016 (32) $[M-3\ \text{monomers}+H]^+$, 899 (100) $[M-\text{Rhod}-Cl]^+$, 888 (56) $[M-4\ \text{monomers}+H]^+$, 760 (52) $[M-5\ \text{monomers}+H]^+$; HR-MS (FAB, matrix: glycerine), *m/z* (%): $C_{42}H_{87}N_{14}O_7$, fragment: 100 $[M-\text{Rhod}-Cl]^+$, calcd 899.6882; found 899.6879.

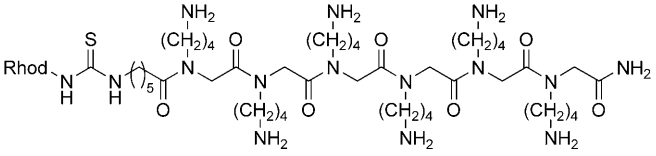

Fluo-{6^G,6^G,6^G,6^G,6^G,6^G}-NH_2 (TS-165):[31] As described in general procedures A1–E1, the product was obtained as an orange solid; yield: 32 mg (59%). MS (FAB, matrix: 3-NBA), *m/z* (%): 1677 (1) $[M]^+$, 1004 (9) $[NH_2+\text{pentamer}-H]^+$, 852 (26) $[NH_2+\text{tetramer}+CH_2N_2]^+$, 810 (18) $[NH_2+\text{tetramer}+H]^+$, 612 (10) $[NH_2+\text{trimer}+H]^+$, 456 (20) $[NH_2+\text{dimer}+CH_2N_2]^+$, 414 (6) $[NH_2+\text{dimer}+H]^+$, 154 (100) $[\text{Matrix}+H]^+$. IR (drift): ν = 3347 (w), 3199 (w), 2945 (w), 2866 (w), 1668 (w), 1471 (w), 1180 (w), 1137 (w), 837 (w), 802 (w), 722 (w). UV/Vis (CH_3OH): λ_{max}, ($\log\varepsilon$) = 193 (4.9), 486 (3.5).

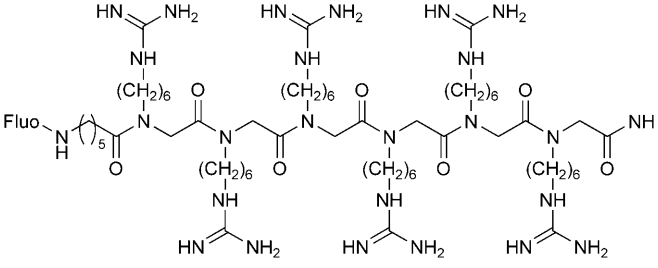

Rhod-{6^G,6^G,6^G,6^G,6^G,6^G}-OH (EB-220): As described in general procedures A2–E2, the product was obtained as a red solid; crude yield: 72 mg (58%). The substance was purified with HPLC; yield after purification 0.44 mg with a HPLC purity of 90%. MS (MALDI, matrix: DHB), *m/z* (%): 1745 $[M]^+$, 1731 [*M* of formylated product]$^+$; two main signals were obtained in a ratio of 1:1 due to formylation of one side chain during guanidinylation.

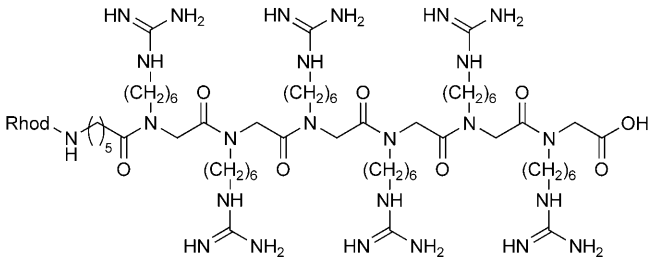

HPLC purification of peptoids: Analytical and preparative HPLC was performed on a chromatographic system from Jasco (Tokyo, Japan) equipped with diode-array detector. Reversed-phase C18 analytical (4.6×250 mm, 5 μm) or semipreparative (10×250 mm, 10 μm) columns from Grace (Grace, Deerfield, IL, USA) were employed for purity assessment and purification, respectively. For chromatographic separation of the peptoids, focused gradients were run from 48 to 56% at a constant temperature of 40 °C. Solvent A: 0.1% trifluoroacetic acid (TFA); B: 90% acetonitrile in 0.1% TFA. The separation of the peptoids was monitored with UV detection in the range 200–650 nm and UV spectra along with MALDI-TOF mass spectrometry were used to identify the product peaks. Manually collected fractions of the semipreparative runs were freeze dried and immediately used in the biological assays. Prior to lyophilization, fraction aliquots were directly reinjected onto the analytical column to quantify purity, which was determined by integration of the respective single peak area from the chromatograms at 220 nm.

Cell lines: The tobacco cell line BY-2 (*Nicotiana tabacum* L. cv. Bright Yellow 2)[32] was cultivated in liquid medium containing Murashige and Skoog salts (4.3 g L^{-1}; Duchefa, Haarlem, The Netherlands), sucrose (30 g L^{-1}), KH_2PO_4 (200 mg L^{-1}), inositol (100 mg L^{-1}), thiamine (1 mg L^{-1}), and 2,4-dichlorophenoxyacetic acid (0.2 mg L^{-1}) at pH 5.8. Cells were subcultured weekly by inoculation of cells in the stationary phase (1.5–2 mL) into fresh medium (30 mL) in Erlenmeyer flasks (100 mL). Cell suspensions were incubated at 25 °C in the dark on an orbital shaker (KS250 basic, IKA Labortechnik, Staufen, Germany) at 150 rpm. Stock BY-2 calli were maintained on media solidified with agar (0.8%, *w/v*) and subcultured monthly. Transgenic cell lines and calli were maintained on the same media supplemented with either hygromycin (15 mg L^{-1}) for cell line BY-2 GF-11 or kanamycin (25 mg L^{-1}) for cell line BY-2 TuA3-GFP. All experiments were performed 4 days after subcultivation.

Treatment of cells: An aliquot (200 μL) from a four day old BY-2 cell culture was transferred to a reaction tube containing sterile culture medium (1 mL). The Trojan peptoids (25 μM) were applied directly onto the cells. After incubation in the dark, excess peptide was removed and cells were washed by using fresh culture medium. For the inhibitor treatments, stock solutions of latrunculin B (Sigma, Taufkirchen, Germany) and oryzalin (Chem Service, West Chester, PA, USA) in DMSO were diluted with culture medium to the final concentrations (500 nM for latrunculin B, 5 μM for oryzalin) and incubated with the cells for 12 h.[33,34] After pretreatment, the Trojan peptoid TS-165 was added and the cells were then incubated for 2 h, as described above. For covisualization of TS-165 and endosomal vesicles, FM4-64[26] (2 μM; Molecular Probes, Steinheim, Germany) was added to the cells immediately after incubation with TS-165, and incubated for a further 5 min, as described above. To inhibit endocytosis, cells were treated with Wortmannin[27] (33 μM; Molecular Probes, Steinheim, Germany) during incubation with TS-165 and FD-4.

Visualization of actin filaments: Actin filaments were visualized after treatment with TS-165 by the method of Kakimoto and Shibaoka[35] modified according to Olyslaegers and Verbelen.[36] After fixation for 10 min in paraformaldehyde (1.8%, *w/v*) in standard buffer (0.1 M PIPES, 5 mM $MgCl_2$, 10 mM EGTA, pH 7.0), the cells were incubated for 10 min in standard buffer containing glycerol (1%, *v/v*). Subsequently, an aliquot of the cell suspension (0.5 mL) was incubated for 30 min with TRITC-phalloidin (0.5 mL, 0.66 μM; Sigma–Aldrich, Taufkirchen, Germany) freshly prepared from a stock solution (6.6 μM in ethanol 96%, *v/v*) by dilution with phosphate buffered saline (PBS; 0.15 M NaCl, 2.7 mM KCl, 1.2 mM KH_2PO_4, 6.5 mM Na_2HPO_4, pH 7.2). Cells were then washed in PBS three times for at least 5 min. To confirm the findings of TS-063 and EB-220 localization in vivo, the tobacco BY-2 cell line GF-11, which stably expresses a fusion construct of the second actin binding domain (ABD2) of the *Arabidopsis thaliana* AtFim1 protein[37] and green fluorescent protein (GFP), was used as reference.

Visualization of microtubules: After incubation with TS-165, as described above, the cells were processed for immunofluorescence in self-made staining chambers by using a nylon mesh of 70 μm pore-width, as published previously.[38] This allowed fast exchange of media and simultaneously prevented the loss of cells during staining. After fixation for 30 min with paraformaldehyde (3.7%, *w/v*) in microtubule stabilizing buffer (MSB: 50 mM PIPES, 2 mM EGTA, 2 mM $MgSO_4$, 0.1% Triton-X-100, pH 6.9) cells were washed in PBS three times for at least 5 min each time to remove excess paraformaldehyde. Subsequently, the cell wall was digested by using Macerozym (1%, *w/v*; Duchefa, Haarlem, The Netherlands) and Pectolyase (0.2%, *w/v*; Fluka, Taufkirchen, Germany) in MSB for 5 min. Again, excess enzyme was washed out for 5 min with PBS. Unspecific binding sites were blocked for 20 min with bovine serum albumin (BSA; 0.5%, *w/v*) diluted in PBS. Directly after being blocked, the cells were transferred into a small volume of the primary antibody. To visualize microtubules, we used a 1:250 dilution in PBS of monoclonal mouse antibody DM1A[39] (Sigma, Taufkirchen, Germany), which recognizes a conserved epitope near the carboxy terminus of α-tubulin. This primary antibody was allowed to bind for 1 h at 37 °C in a moist chamber to prevent desiccation of the specimen. Immediately thereafter, unbound primary antibody was removed by washing the cells three times for at least 5 min each time in PBS. The sample was then incubated with a secondary FITC-conjugated antibody targeted against mouse IgG for 1 h at 37 °C in a moist chamber. Unbound secondary antibody was removed by washing with PBS. To verify our findings, we used the BY-2 cell line TuA3–GFP expressing a fusion construct of the tobacco tubulin TuA3 with GFP.[40]

Microscopy and quantification of uptake: Samples were examined under an AxioImager Z.1 microscope (Zeiss, Jena, Germany) equipped with an ApoTome microscope slider for optical sectioning and a cooled digital CCD camera (AxioCam MRm). For the observation of TRITC fluorescence and FM4-64, filter set 43 HE (excitation at 550 nm, beamsplitter at 570 nm, and emission at 605 nm) was used. FITC and GFP fluorescence were viewed through filter set 38 HE (excitation at 470 nm, beamsplitter at 495 nm, emission at 525 nm; Zeiss, Jena, Germany). The images were analyzed by using the Axio-Vision (release 4.5) software and processed for publication by using Photoshop (Adobe Systems, San Jose, CA, USA). For the quantification of uptake, cell suspension (200 μL) and culture medium (1 mL) were mixed in a reaction tube (1.5 mL). The Trojan peptoid TS-165 or the 4 kDa FITC-labeled dextrane FD-4 (Sigma–Aldrich, Taufkirchen, Germany) were then added to the final concentrations (25 μM). The mixture was then incubated on

an orbital shaker (KS250 basic, IKA Labortechnik, Staufen, Germany) in the dark at 150 rpm for specified time intervals (ranging from 15 min to 20 h). After incubation, the cells were transferred into self-made staining chambers by using a nylon mesh of 70 μm pore-width to allow easy drainage of the fluorescent markers, thoroughly rinsed with sterile culture medium, and viewed immediately. For the quantification of uptake, time series of black and white images were recorded and analyzed for each time point by using the Image J software (http://rsb.info.nih.gov/ij/). Image acquisition parameters were standardized with respect to time of exposure and adjustment of brightness, contrast and gamma correction to allow for quantitative comparison of the uptake of both TS-165 and FD-4. For each individual image, brightness was corrected for background brightness from a reference area outside of the target cells, and then the fluorescence intensity was averaged over the cell interior by using the freehand selection tool of the software. For each time point, 167 to 245 individual cells from two independent experimental series were evaluated.

Acknowledgements

This work was supported by the Center for Functional Nanosciences of the German Research Council (projects E1.1 and E1.5), a fellowship from the State of Baden–Württemberg (Landesgraduiertenförderprogramm) to T.S. and a fellowship from the German Business Foundation (Stiftung der Deutschen Wirtschaft) to E.B. Technical help from Sabine Purper in the cultivation of the cell lines is gratefully acknowledged as is assistance from Sergii Afonin during HPLC purification.

Keywords: drug delivery · peptidomimetics · peptoids · plant cells · tobacco BY-2 cells

[1] A. D. Frankel, C. O. Pabo, *Cell* **1988**, *55*, 1189–1193.
[2] M. Green, P. M. Loewenstein, *Cell* **1988**, *55*, 1179–1188.
[3] P. A. Wender, D. J. Mitchell, K. Pattabiraman, E. T. Pelkey, L. Steinman, J. B. Rothbard, *Proc. Natl. Acad. Sci. USA* **2000**, *97*, 13003–13008.
[4] S. Fawell, J. Seery, Y. Daikh, C. Moore, L. L. Chen, B. Pepinsky, J. Barsoum, *Proc. Natl. Acad. Sci. USA* **1994**, *91*, 664–668.
[5] R. B. Pepinsky, E. J. Androphy, K. Corina, R. Brown, J. Barsoum, *DNA Cell Biol.* **1994**, *13*, 1011–1019.
[6] E. Vives, P. Charneau, J. van Rietschoten, H. Rochat, E. Bahraoui, *J. Virol.* **1994**, *68*, 3343–3353.
[7] E. Vives, P. Brodin, B. Lebleu, *J. Biol. Chem.* **1997**, *272*, 16010–16017.
[8] D. Derossi, A. H. Joliot, G. Chassaing, A. Prochiantz, *J. Biol. Chem.* **1994**, *269*, 10444–10450.
[9] G. Elliott, P. Ohare, *Cell* **1997**, *88*, 223–233.
[10] M. Lindgren, M. Hallbrink, A. Prochiantz, U. Langel, *Trends Pharmacol. Sci.* **2000**, *21*, 99–103.
[11] K. T. Jeang, H. Xiao, E. A. Rich, *J. Biol. Chem.* **1999**, *274*, 28837–28840.
[12] H. Nagahara, A. M. Vocero-Akbani, E. L. Snyder, A. Ho, D. G. Latham, N. A. Lissy, M. Becker-Hapak, S. A. Ezhevsky, S. F. Dowdy, *Nat. Med.* **1998**, *4*, 1449–1452.
[13] M. Rueping, Y. R. Mahajan, B. Jaun, D. Seebach, *Chem. Eur. J.* **2004**, *10*, 1607–1615.
[14] G. M. Figliozzi, R. Goldsmith, S. Ng, S. C. Banville, R. N. Zuckermann, *Methods Enzymol.* **1996**, *267*, 437–447.
[15] S. M. Miller, R. J. Simon, S. Ng, R. N. Zuckermann, J. M. Kerr, W. H. Moos, *Drug Dev. Res.* **1995**, *35*, 20–32.
[16] R. J. Simon, R. S. Kania, R. N. Zuckermann, V. D. Huebner, D. A. Jewell, S. Banville, S. Ng, L. Wang, S. Rosenberg, *Proc. Natl. Acad. Sci. USA* **1992**, *89*, 9367–9371.
[17] I. Peretto, R. M. Sanchez-Martin, X. H. Wang, J. Ellard, S. Mittoo, M. Bradley, *Chem. Commun.* **2003**, 2312–2313.
[18] M. A. Fara, J. J. Díaz-Mochón, M. Bradley, *Tetrahedron Lett.* **2006**, *47*, 1011–1014.
[19] J. R. Holder, R. M. Bauzo, Z. Xiang, J. Scott, C. Haskell-Luevano, *Bioorg. Med. Chem. Lett.* **2003**, *13*, 4505–4509.
[20] T. Uno, E. Beausoleil, R. A. Goldsmith, B. H. Levine, R. N. Zuckermann, *Tetrahedron Lett.* **1999**, *40*, 1475–1478.
[21] J. A. W. Kruijtzer, L. J. F. Hofmeyer, H. Wigger, C. Versluis, R. M. J. Liskamp, *Chem. Eur. J.* **1998**, *4*, 1570–1580.
[22] K. Simons, D. Toomre, *Nat. Rev. Mol. Cell Biol.* **2000**, *1*, 31–41.
[23] A. K. Grennan, *Plant Physiol.* **2007**, *143*, 1083–1085.
[24] M. Uemura, R. A. Joseph, P. L. Steponkus, *Plant Physiol.* **1995**, *109*, 15–30.
[25] T. Mizuno, M. Miyashita, H. Miyagawa, *J. Pept. Sci.* **2009**, *15*, 259–263.
[26] P. Dhonukshe, J. Mathur, M. Hülskamp, T. W. Gadella, Jr., *BMC Biol.* **2005**, *3*, 11–26.
[27] N. Emans, S. Zimmermann, R. Fischer, *Plant Cell* **2002**, *14*, 71–86.
[28] I. Spector, N. R. Shochet, D. Blasberg, Y. Kashman, *Cell Motil. Cytoskeleton* **1989**, *13*, 127–144.
[29] K. Mizuno, T. Suzuki, *Bot. Mag. Tokyo* **1990**, *103*, 435–448.
[30] T. Schröder, K. Schmitz, N. Niemeier, T. S. Balaban, H. F. Krug, U. Schepers, S. Bräse, *Bioconjugate Chem.* **2007**, *18*, 342–354.
[31] T. Schröder, N. Niemeier, S. Afonin, A. S. Ulrich, H. F. Krug, S. Bräse, *J. Med. Chem.* **2008**, *51*, 376–379.
[32] T. Nagata, Y. Nemoto, S. Hasezawa, *Int. Rev. Cytol.* **1992**, *132*, 1–30.
[33] J. Maisch, J. Fišerová, L. Fischer, P. Nick, *J. Exp. Bot.* **2009**, *60*, 603–614.
[34] K. Schwarzerová, J. Petrášek, K. C. S. Panigrahi, S. Zelenková, Z. Opatrný, P. Nick, *Protoplasma* **2006**, *227*, 185–196.
[35] T. Kakimoto, H. Shibaoka, *Protoplasma* **1987**, *140*, 151–156.
[36] G. Olyslaegers, J. P. Verbelen, *J. Microsc.* **1998**, *192*, 73–77.
[37] T. Sano, T. Higaki, Y. Oda, T. Hayashi, S. Hasezawa, *Plant J.* **2005**, *44*, 595–605.
[38] P. Nick, A. Heuing, B. Ehmann, *Protoplasma* **2000**, *211*, 234–244.
[39] F. Breitling, M. Little, *J. Mol. Biol.* **1986**, *189*, 367–370.
[40] F. Kumagai, A. Yoneda, T. Tomida, T. Sano, T. Nagata, S. Hasezawa, *Plant Cell Physiol.* **2001**, *42*, 723–732.

Received: May 28, 2009
Published online on September 8, 2009

